

Question 2: Chapter 1 of the book introduces an example of a pattern classification system that distinguishes sea-bass from salmon. Present a different example of a pattern classification system which may be of some commercial use. Choose a classification problem for which you can actually collect a few training samples (5 samples per class) and measure features on them. Briefly describe the (i) pattern classes, (ii) transducer to be used, (iii) preprocessing and segmentation routines, and (iv) features that may separate these two classes. Why would you be interested in automating this classification problem?

Select two important features for this problem and show the 1-dimensional histograms (class-conditional densities) for these two features (see Figures 1.2 and 1.3 of the book). Also show the 2-dimensional scatter plot when both features are used simultaneously. Are the pattern classes reasonably well-separated in the 2D feature space that you have chosen?

(i) Classification Problem

The liver is the largest organ inside the body. It lies under the right ribs, just below the right lung. If you were to poke your fingers up under your right ribs, you would almost be touching your liver.

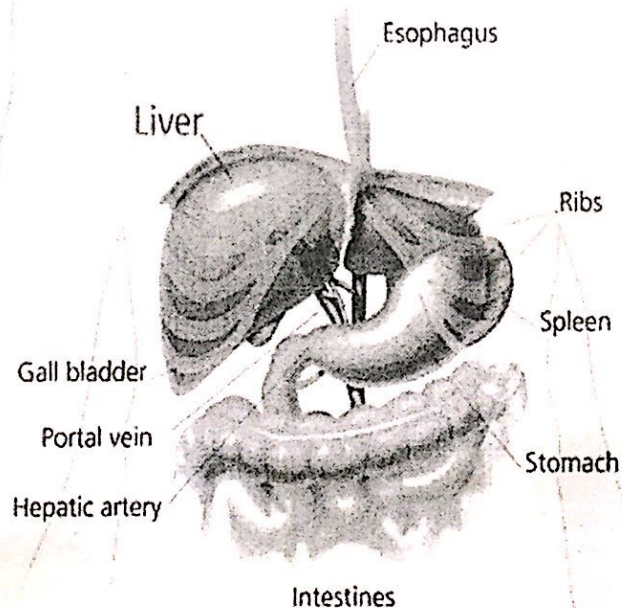


Figure 2.1: Anatomy of the Abdomen.

The liver is shaped like a pyramid and is divided into right and left lobes. Unlike most other organs, the liver gets blood from 2 sources. The hepatic artery supplies the liver with blood that is rich in oxygen. The portal vein carries nutrient-rich blood from the intestines to the liver.

The liver has many vital functions:

- It breaks down and stores many of the nutrients absorbed from the intestine.
- It makes some of the clotting factors needed to stop bleeding from a cut or injury.
- It secretes bile into the intestine to help absorb nutrients.
- It plays an important part in removing toxic wastes from the body.

Because the liver is made up of several different types of cells, many types of tumors can form in the liver. Some of these are cancerous and some are not cancerous. The medical word for tumors that are not cancer is benign (be-nine). These tumors have different causes and are treated different ways. The outlook for your health or recovery depends on what type of tumor you have.

1. Benign Tumors

Benign tumors can sometimes grow large enough to cause problems, but most of the time they do not go into nearby tissues or spread to distant parts of the body. If they need to be treated, they can usually be cured by removing them during surgery.

2. Malignant Tumors

They are commonly defined as cancer. They are generally more serious and may be life threatening. Cancer cells can invade and damage nearby tissues and organs. Also, cancer cells can break away from a malignant tumor and enter the bloodstream or the **lymphatic system**. That is how cancer cells spread from the original cancer (the **primary tumor**) to form new tumors (**secondary tumors**) in other organs. Different types of cancer tend to spread to different parts of the body.

Secondary Liver Cancer

Most of the time when cancer is found in the liver it did not start there but spread to the liver from a cancer that began somewhere else in the body. These tumors are named after the place where they began (the primary site) and are further described as *metastatic*. For example, cancer that started in the lung and spread to the liver is called metastatic lung cancer to the liver. The rest of the information given here covers only primary liver cancer, that is, cancer that *starts* in the liver.

(ii) Pattern Classes

In this study we will try to classify 2 types of Ct images for the liver,

- 1- Normal liver



Figure 2.2 Normal liver

- 2- Hepatic Metastasis: When liver cancer spreads metastasis outside the liver, the cancer cells tend to spread to nearby lymph nodes and to the bones and lungs. When this happens, the new tumor has the same kind of abnormal cells as the primary tumor in the liver. For example, if liver cancer spreads to the bones, the cancer cells in the bones are actually liver cancer cells. The disease is metastatic liver cancer, not bone cancer. It is treated as liver cancer, not bone cancer. Doctors sometimes call the new tumor "distant" disease. Similarly, cancer that spreads to the liver from another part of the body is different from primary liver cancer. The cancer cells in the liver are like the cells in the original tumor. When cancer cells spread to the liver from another organ (such as the colon, lung, or breast), doctors may call the tumor in the liver a secondary tumor. In the United States, secondary tumors in the liver are far more common than primary tumors.

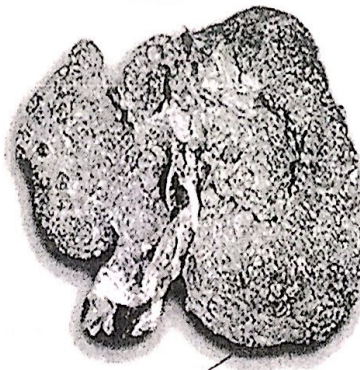


Figure 2.3 Hepatic Metastasis liver

- 3- Hepatic adenoma (HA) is a rare benign tumor of the liver. Two types of HAs have been identified, including tumors of bile duct origin and tumors of liver cell origin. HAs of bile duct origin usually are smaller than 1 cm and not of clinical interest; typically, they are found incidentally on postmortem examinations. HAs of liver origin are larger and often are clinically significant. On average, they measure 8-15 cm²

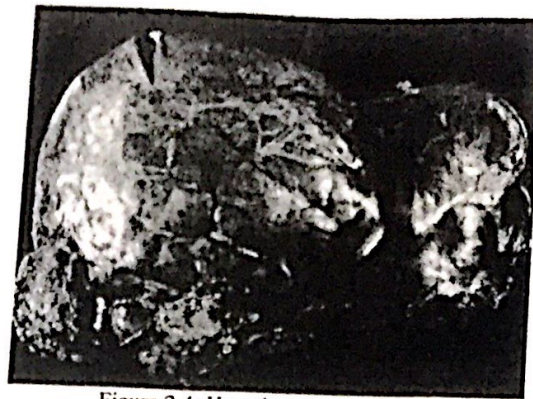


Figure 2.4: Hepatic Adenoma Liver.

(iii) Input Sensor

The differentiating between tumored liver and normal liver is just made using helical CT or MRI, but to diagnose if the tumor is malignant or benign, this needs mostly to use both modalities to image, but to take the final diagnosing decision, it is a must to take a biopsy ensure the imaging results taken or to contradict them, which makes this issue a hot research topic to work in these days. The output of Medical Imaging Equipment are images saved as Digital Imaging and communication format, "DICOM" files, which can be ready now for processing

But, in this study, I will just take helical CT images to somehow differentiate between the three types of livers. So the **input sensor** will be the CT imaging machine.

(iv) Preprocessing and Segmentation

Here are some CT images for the three types of images we want to classify:

1- Normal liver

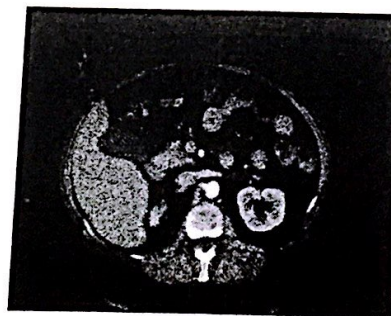
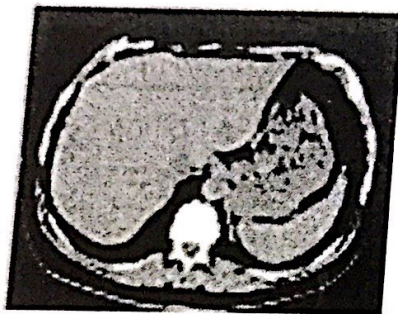


Figure 2.5: CT sample images for Normal Liver.

2- Hepatic Metastasis

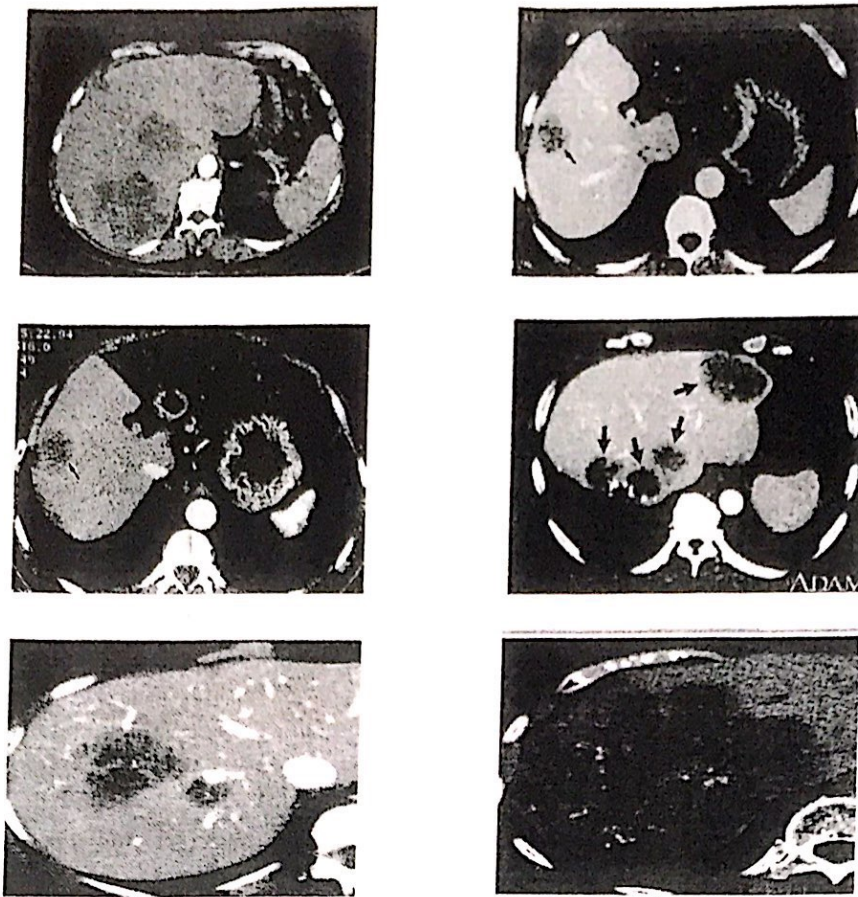


Figure 2.6: CT sample images for Hepatic Metastasis Liver.

3- Hepatic adenoma



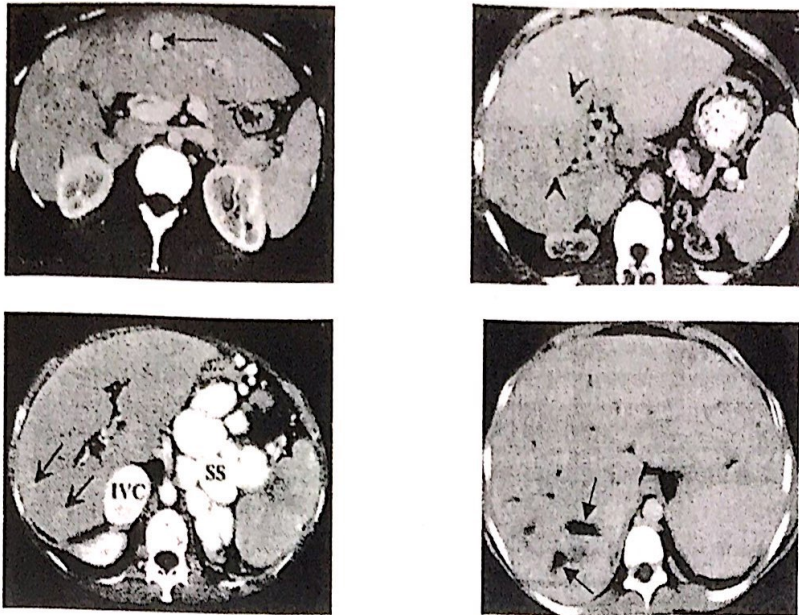


Figure 2.7: CT sample images for Hepatic Adenoma Liver.

(v) Preprocessing and Segmentation

Liver segmentation is one of the most basic and important parts in computer-aided diagnosis for liver CT. A number of automatic or semiautomatic segmentation methods in a variety of human organs for various purposes have been reported. Bae et al (5) developed a system based on gray-level thresholding, Gaussian smoothing, and eight-point connectivity tracking for automatic liver structure segmentation in surgical planning of living-donor liver transplants. Their images, however, were obtained in the equilibrium phase after intravenous infusion of iodinated contrast material. Brummer et al (6) used analysis of gray-level histograms and mathematic morphologic methods for automatic segmentation of magnetic resonance images of the brain. Philip et al (7) described a method for the automatic detection of myocardial contours from cine CT cardiac images. Williams et al (8) reported a technique for the segmentation of liver tumor from a userdefined region of interest that contained the tumor. Many other efforts to segment medical images can also be found (9-14). Despite these efforts, there are still no automatic segmentation methods that are generally applicable and that can be used for the purpose of 3D visualization of the liver. The difficulty comes from multiple sources that include limited contrast between the liver and surrounding tissues, the variety of human liver geometric properties and contrast enhancement kinetics from case to case, the requirement of including both tumors and vasculature in the segmented liver, and image noise.

The most reliable proposed scheme is carried out on region-of-interest (ROI) blocks that include regions of the liver with high probabilities. These methods utilize the composition of morphological filters with a priori knowledge, such as the general location or the approximate intensity of the liver to detect the initial boundary of the liver. Then, they use the gradient image with the weight of an initial liver boundary and segment the liver region by using an immersion-based watershed algorithm in the gradient image. Finally, a refining process is carried out to acquire a more accurate liver region. The other way which is also proposed is to use the matter of stochastic processes

because of the large variation of the liver size form a person to another and from normal to abnormal case.

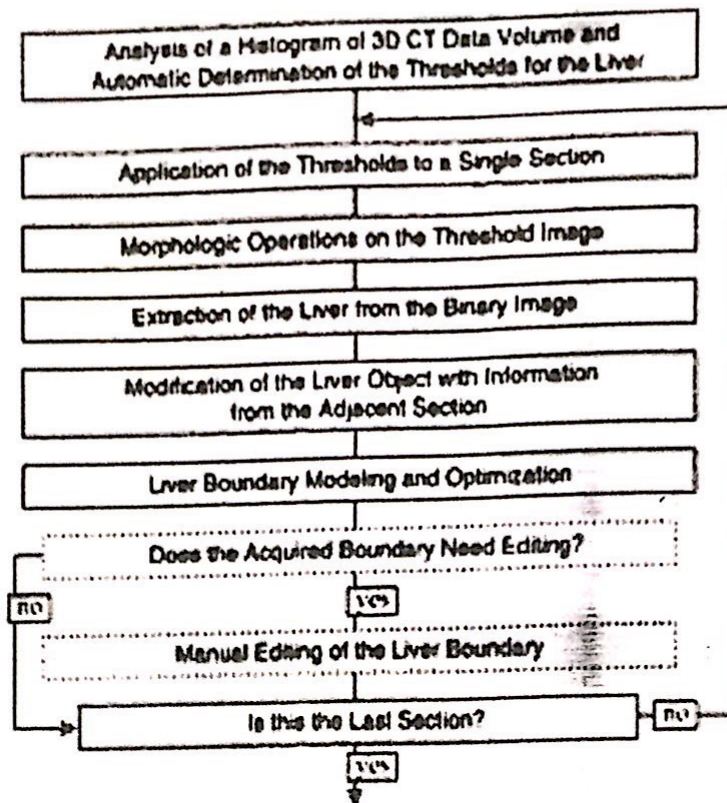


Figure 2.8: Flow diagram shows the automatic liver segmentation algorithm. Dashed blocks indicate where user interactions can occur.

Here, I will present a method which gave good result in segmentation of the liver, this algorithm relies on focusing The attention on liver images obtained with use of two different protocols: helical CT during arterial portography (CTAP) and helical CT with use of intravenous contrast material. Data sets acquired with use of these protocols contain a 3D volume of the liver and adjacent organs. The gray levels of the liver usually overlap those of other tissues. Furthermore, the gray levels of the liver may vary from section to section depending on the speed and timing of data acquisition.⁴ This automated algorithm begins with the analysis of the gray-level histogram for the CT image and continues by iterating through each section. Analysis of the histogram, together with thresholding and morphologic operations, results in an initial estimate of a liver boundary. Information from adjacent sections is used to modify the estimated boundary. The boundary is then further refined by using edge information in the image. This final step is achieved by first representing the boundary with use of the parametrically deformable contour model, and then matching the model to an edge enhanced image through optimization. User modification of the output boundary can be made after a single section has been segmented (dashed blocks in Figure 1), or it can be applied after all sections have been segmented by the automatic algorithm. By using both gray-level distribution analysis and edge detection, it is reasonable to expect the algorithm to perform better than use of either method alone.

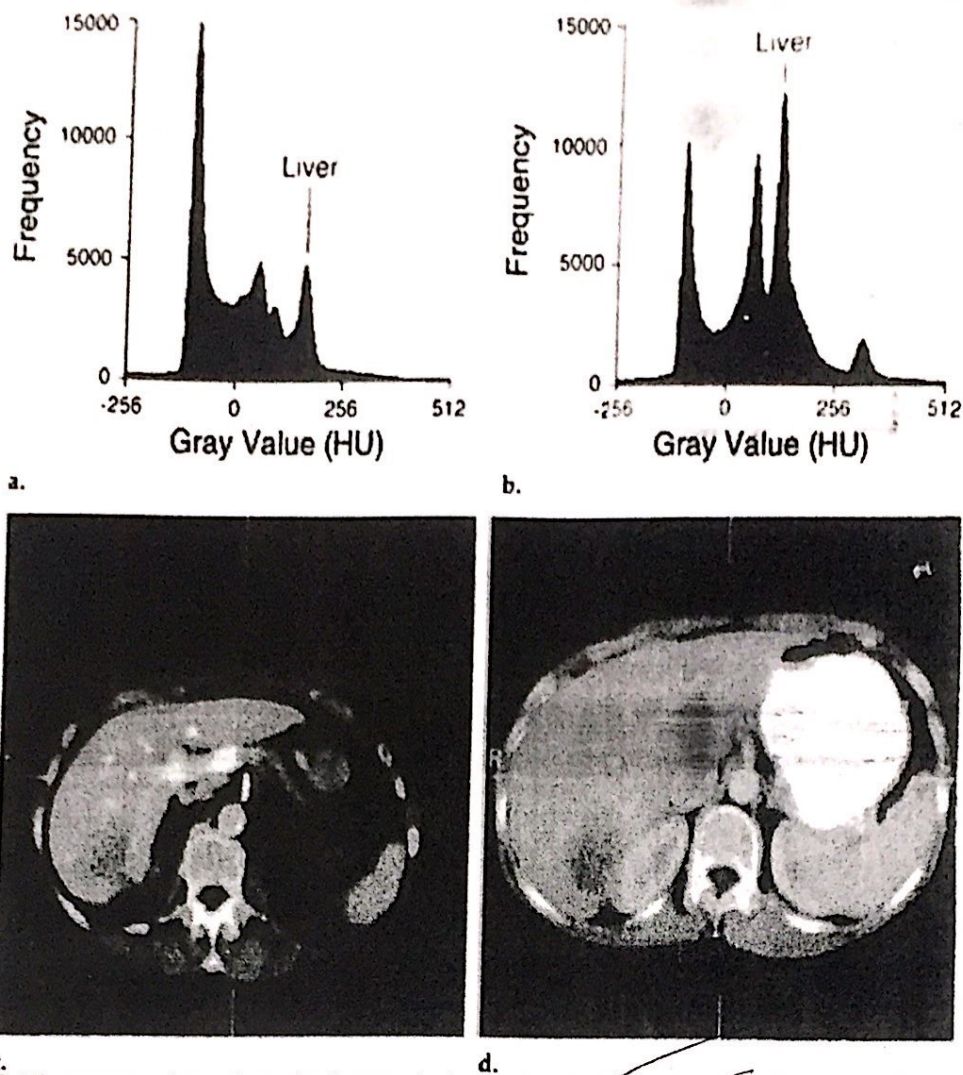


Figure 2.9. Histograms and sample section images obtained at CTAP of the abdomen and contrast-enhanced CT data sets. (a) Histogram shows a 3D CTAP data set. (b) Histogram shows a 3D contrast-enhanced CT data set. (c) Image from the data set acquired at CTAP. (d) Image from the contrast-enhanced CT data set. Note that the air portion of the histogram is not shown and the gray-level units are given in Hounsfield units (HU).

The first step in our automated technique is analysis of the gray-level histogram for the whole volume and thresholding of each section. Representative histograms of a CTAP scan and a contrast enhanced CT data set are shown in Figure 2.9a and 2.9b. The peak corresponding to the liver in each of the images is indicated in the figure. This peak position can be located by using the technique which automatically searches for the liver peak by exploiting information that concerns both the amplitudes and the gray-level range of the peaks. The two thresholds for the liver were determined by two offsets from the peak based on the standard deviation (SD) of the gray level of the liver. The intracase gray-level SD of the liver is approximately 13 HU. The initial lower and upper thresholds for CTAP images are chosen as 2 SDs less than and 3 SDs greater than the peak value, respectively. For contrast-enhanced CT images, the lower threshold is 3 SDs less than the peak value and the upper threshold is 2 SDs greater than the peak value.

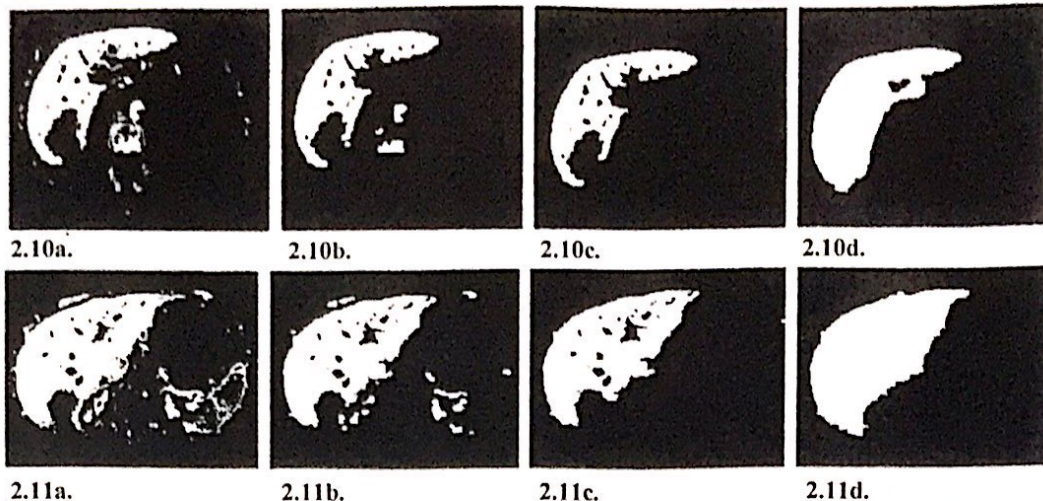


Figure 2.10 & 2.11: Binary images that result from the steps of the algorithm applied to the (CTAP image in Figure 2.9c and (4) contrast-enhanced CT image in Figure 2.9d. (2.10a, 2.11a) Thresholding of the original image. (2.10b, 2.11b) Opening of the threshold image. (2.10c, 2.11c) Extraction of the object with maximum area. (2.10d, 2.11d) Liver objects obtained by using information from adjacent sections and addition of vessels.

As seen in Figure 2.9c and 2.9d, kidneys are usually less attenuating (have lower CT numbers and thus appear darker) than the liver on CTAP images and the kidneys are usually more attenuating (brighter) than the liver on contrast-enhanced CT images. Although there is some flexibility in the choice of the upper threshold for a CTAP image or the lower threshold for a contrast-enhanced CT image, the lower threshold for a CTAP image and the upper threshold for a contrast-enhanced CT image are more crucial in that they affect the number of pixels that connect the liver and kidney. The remaining thin connection between the liver and kidney can usually be broken by steps described in the following sections. Figure 2.10a and 2.11a show examples of the binary images that resulted from thresholding the images in Figure 2.9c and 2.9d. The liver vasculature (which has higher CT numbers than those of liver) and tumors (which usually have lower CT numbers than those of liver) cause holes in the binary images. Therefore, the vasculature and tumors need to be delineated and added to the liver image. A second binary image was obtained by thresholding the original image between the upper liver threshold and the maximum possible gray level. The resulting image contains hepatic vasculature and other tissues with higher gray levels. This image is processed to determine which objects represent vessels on the basis of their shapes and positions; those that do are combined with the liver.

Morphologic Operations

After thresholding, the liver may still be connected with neighboring tissues that have similar gray levels (Figs 2.10a, 2.11a). Mathematic morphologic operations, specifically erosion or opening, can be used to remove thin connections, and dilation or closing can be used to fill narrow gaps between fragments. We used an opening operation to break the connections between the liver and kidneys. Morphologic operations are described by the shape and size of the structural element used. These shapes are generally symmetric to the coordinate axes. When an opening or erosion operator is used, the size of the structural element has to be chosen carefully. If the structural element is too small, undesired connections that are thicker than the diameter of the element cannot be broken.



Figure 2.12: CT image of the final liver boundaries obtained by optimization of the parametrically deformable contour model and superimposed on the original images shown in Figure 2.9c and 2.9d. The image (a) corresponds to Figure 2.9c, and (b) corresponds to Figure 2.9d.

On the other hand, a structural element that is too large causes numerous undesired fragments and can adversely affect the liver shape. We used a circular structural element with a diameter of 5 pixels for the opening operation. This value was determined empirically. For those connections between the liver and its surrounding tissues that cannot be broken by the opening operation, additional operations, which are described later, can still be expected to correct the error. Figures 3b and 4b show the results of applying the opening operation to the images shown in Figures 2.10a and 2.11a. Extraction of the Liver Object After the thresholding and opening operations, the liver is usually the object with a maximum area in each section (except in sections very close to the superior or the inferior portions of the liver, where the spleen or other tissues may have a larger area than that of liver). Therefore, by comparing the area of each connected part and retaining only the one with a maximum area, the liver can be extracted from the image. In sections from the inferior portion of the liver, however, the left and right lobes of the liver may be separate from each other. After first locating the right lobe, which usually has a relatively larger area than that of the left lobe, the algorithm searches in a small area near the medial border of the right lobe to determine if there is a separate left lobe. If a left lobe is found, the two lobes are then connected by growing one toward the other. For any number of reasons, the previous steps may fail. For example, in inferior and superior aspects of the liver, the largest object may not represent the liver. In some cases, the liver may be broken into several parts after thresholding because of the exclusion of tumors or blood vessels. In these cases, information from adjacent, already segmented sections is used to correct these errors. This step is detailed in the next section. The extracted objects from images in Figures 2.10b and 2.11b are shown in Figures 2.10c and 2.11c.

The outcome of the previous steps relies mainly on the uniformity of pixel properties, such as pixel gray levels, within the liver. The next step attempts to improve the accuracy of the liver boundary with use of the edges of the liver, which are characterized by discontinuity of the pixel gray levels. In this step the liver shape is converted to a contour and represent that contour with use of the parametrically deformable contour model, which smoothes the contour by representing the contour with use of a truncated Fourier series of ellipses. It then fits the contour to local edge information in the image. Because the previous steps usually result in a fairly accurate liver boundary, the parametrically deformable contour model typically makes only minor perturbations to the liver

contour. Figure 2.12 shows the acquired liver boundaries superimposed on the original images in Figure 2.9c and 2.9d.



Figure 2.11: Extracted liver of figure 2.9d

(vi) Features Selection

From the medical background, we can find that the tumored liver is much bigger in size than the normal one, and so to fit in areas found between ribs and other organs, its shape won't be uniform as normal, so **contour smoothness** is taken as the second feature. In liver CT, we can find that there are blood vessels viewed in each slice, so the color of the whole liver in case of normal liver is not only one, but in case of tumored liver, 2 new things will appear, first the number of **blood vessels** will increase a lot in this part, secondly new objects with other **gray levels** will appear. So, the histogram will be then calculated and the **histogram standard deviation** from the max peak gray level, **number of gray level peaks within the histogram**, which is estimated to be 2 peaks in case of normal liver, and more in case of tumored one, and the **texture** will be then used as third, fourth and fifth features. The more interesting feature that can be used to differentiate between the hepatic metastasis and the hepatic adenoma is the number of tumors, or **object found**, and their size, it is very known that the size of the malignant tumor is huge and increasing very fast with respect to benign one and that the benign is more spread, which means that you can find lots of small cancerous objects spread within a certain area. So the size of the cyst and the number of cysts found will be the sixth and seventh features.

Now to summarize the features used in the classifications

- 1- liver size.
- 2- contour smoothness.
- 3- number gray level histogram peaks.
- 4- gray level histogram standard deviation.
- 5- Texture.
- 6- Average size of cyst, in case of having multi cysts.
- 7- Number of cysts.

In this study I will use the size of the liver measured as the area of the liver in the image and the contour smoothness to differentiate between normal and tumor liver

And I will use the cyst size versus the number of cysts to differentiate between the hepatic metastasis and the hepatic adenoma.

1- Size of the liver

Size of the normal liver is : The average measured liver diameter (midclavicular line) \pm SD was 14.0 ± 1.7 cm (median, 13.9 cm; range, 9.4-21.3 cm; average in male subjects, 14.5 ± 1.6 cm; and average in female subjects, 13.5 ± 1.7 cm). , the tumored liver size can be of same size of the normal liver in early tumor detection and its size an increase till getting 45 cm^2

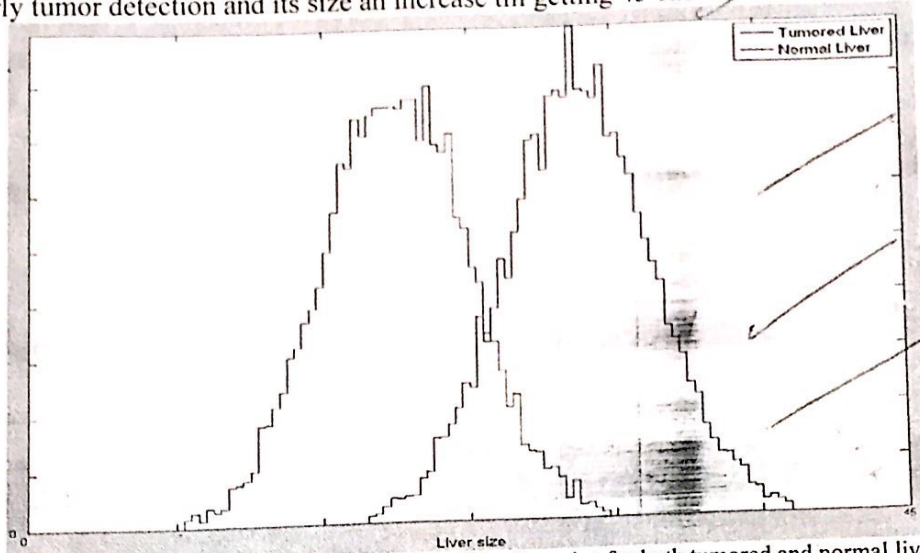


Figure 2.12: Conditional Probability density of the liver size for both tumored and normal liver

2- Smoothness of contour:

It varies form zero in case of smoothed contour, for normal liver , and increases to 1 in case of totally irregular contour shape

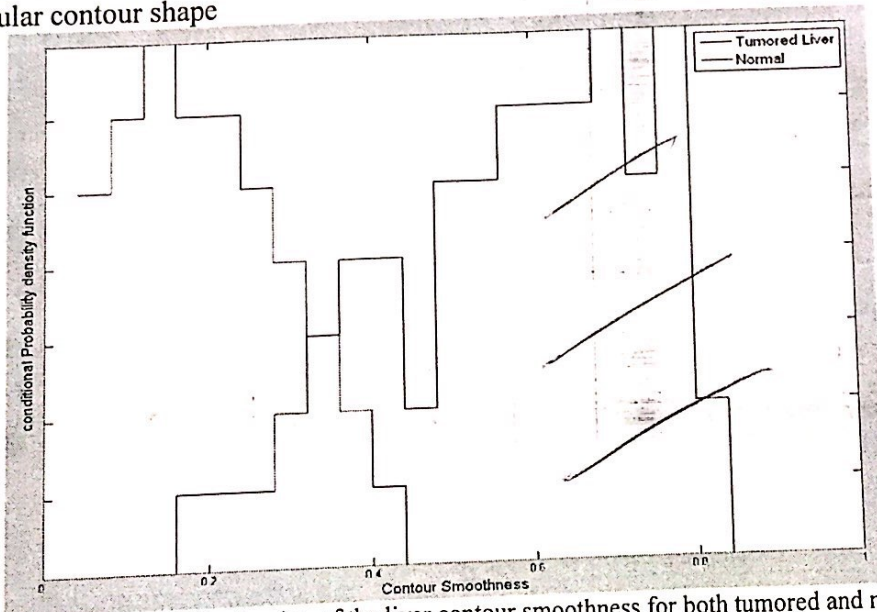


Figure 2.13: Conditional Probability density of the liver contour smoothness for both tumored and normal liver

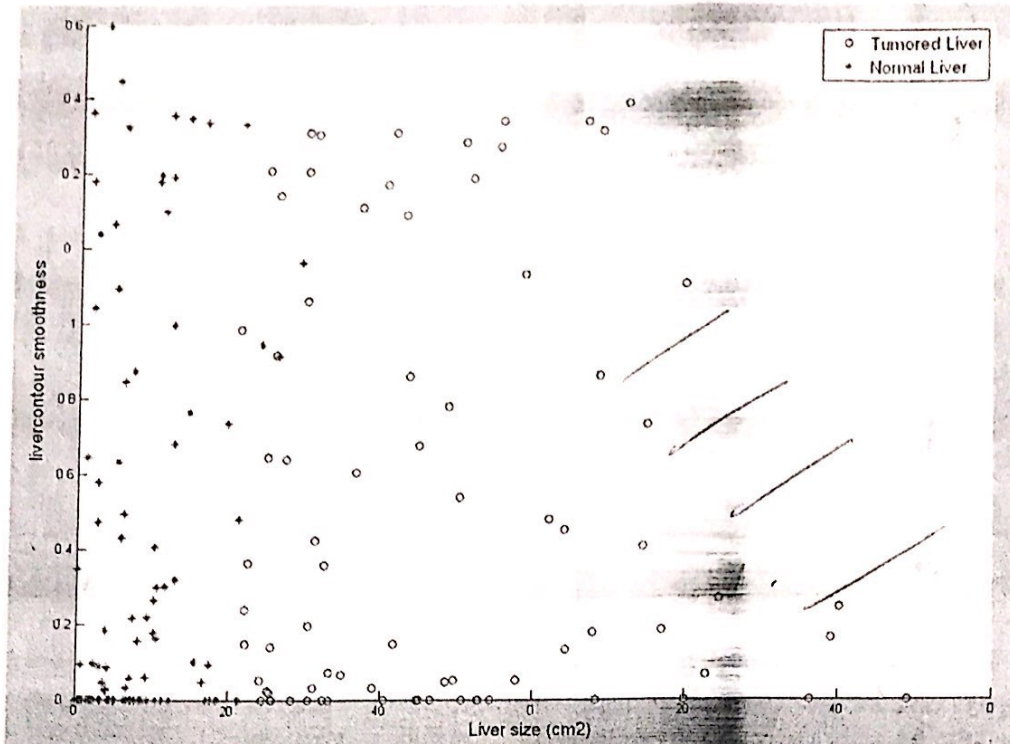


Figure 2.13: Conditional Probability density of the liver contour smoothness for both tumored and normal liver

From the previous scatter plot, it is very clear that these features are somehow enough to make a complete classification for the tumored and normal liver, but the gray level distribution is a key to be used to increase the accuracy and decrease the complexity of the boundary needed for classification

Tumor type Classification

Next step after the classifying the liver as a tumored liver, need to be classified as hepatic adenoma or hepatic metastasis, I will use the two following features for classification

1- Average Size of the cyst

Next step after the classifying the liver as a tumored liver, need to be classified as hepatic adenoma or hepatic metastasis, I will use the two following features for classification

2- Number of cysts

Size of the cyst

The size of the hepatic adenoma cysts varies from 8 to 15 cm², but that of the hepatic metastasis varies from 10 to 40 cm², figure 2.12 represents a methodology to measure the cyst area

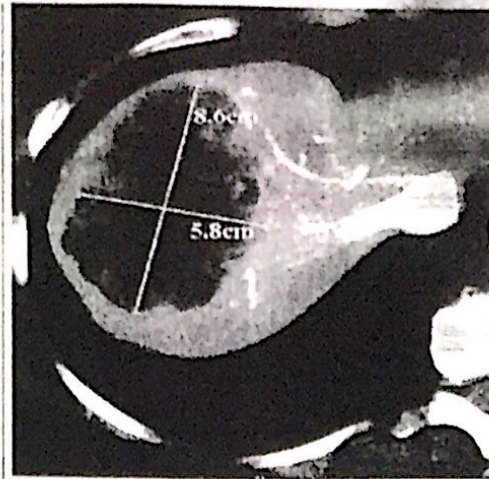


Figure 2.12: shows measurement of a cyst to calculate its area.

We can then use the same manner to plot the conditional densities of both types of tumors and the scatter plot.

References

- (1) <http://www.issoonline.com/content/4/1/17/>
- (2) Luigi Grazioli, Michael P. Federle, Giuseppe Brancatelli, Tomoaki Ichikawa, Lucio Olivetti, Arye Blachar, "Hepatic Adenomas: Imaging and Pathologic Findings", *RadioGraphics* 2001; 21:877-894
- (3) <http://www.issoonline.com/content/4/1/17/>
- (4) Luomin Gao, DAvid G. Heath, Brian S. Kuszyk, Elliot K. Fishman, "Automatic Liver Segmentation Technique for Three-dimensional Visualization of CT Data" *Radiology* 1996; 201:359-364
- (5) Factors Affecting Liver Size
- (6) Schwartz LH, Gandras EJ, Colangelo SM, *et al.* "Prevalence and importance of small hepatic lesions found at CT in patients with cancer". *Radiology* 1999; 210: 71-74.
- (7) Junsung Choi, MD, "Imaging of Hepatic Metastases". *Cancer control*, 2006; 13:1-12.
- (8) www.info-radiologie.ch/abdominal_ct.php
- (9) www.netmedicine.com/xray/ctscan/ct.htm
- (10) www.cancer.org/docroot/CRI/content/CRI_2_4_3X_How_is_liver_ccancer_diagnosed_25.asp
- (11) radiology.rsna.org/cgi/content/figonly/213/3/825
- (12) health.allrefer.com/pictures-images/liver-metastases-ct-scan.html
- (13) brighamrad.harvard.edu/Cases/bwh/hcache/386/full.html
- (14) www.nlm.nih.gov/medlineplus/ency/article/003789.htm
- (15) www.medhelp.org/Medical-Dictionary/Terms/1/003789.htm
- (16) adam.about.com/encyclopedia/Abdominal-CT-scan.htm

20

V. Good